Bioactivity and Mechanical Property of PMMA Bone Cement: Effect of Silanized Mesoporous Borosilicate Bioglass Microspheres

NI Xiaoshi, LIN Ziyang, QIN Muyan, YE Song, WANG Deping

(School of Materials Science and Engineering, Tongji University, Shanghai 201804, China)

Abstract: Poly(methyl methacrylate) (PMMA) bone cement is widely used in orthopaedic surgery as an injectable artificial bone repair material due to its advantages such as desirable mechanical properties, suitable curing time and low toxicity. However, its bioinert polymer may lead to aseptic loosening of the prostheses after long-term implantation. Here, silanized mesoporous borosilicate bioglass microspheres (MBGSSI) composite with PMMA bone cement was prepared to obtain ideal bone repair material with desirable bioactivity and mechanical properties. Mesoporous borosilicate bioglass microspheres (MBGS) were prepared by template method and modified by silane coupling agent γ-methylacryloxy propyl trimethoxysilane (γ-MPS) to obtain MBGSSI. The results indicated that MBGSSI possessed increased specific surface area and decreased total pore volume than MBGS did by the binding between γ-MPS and MBGS occurred on the near surface of mesoporous microspheres. Compared with MBGS/PMMA, MBGSSI/PMMA composite bone cements demonstrated improved mechanical properties, which met the mechanical properties requirements of ISO 5833:2002 because γ-MPS improved the combination between inorganic and organic phases of composite. In addition, the hydroxyapatite (HA) could widely form on the surface of both MBGS/PMMA and MBGSSI/PMMA composite bone cements after immersing in SBF for 42 d, demonstrating the excellent bioactivity. Hence, it is suggested that MBGSSI/PMMA can be a potential bone repair material.

Key words: bioglass; silanization; PMMA bone cement; bioactivity; mechanical property

PMMA bone cement is widely used in orthopaedic surgery as an injectable artificial bone repair material due to its advantages such as desirable mechanical properties, suitable curing time and low toxicity[1]. However, the bioinert polymer may lead to the aseptic loosening of the prostheses after long-term implantation, and the high polymerization temperature reaching 70–110 ℃ causes thermal damage to surrounding cells and tissues as well[2-3]. The addition of bioactive materials serves as an effective way to improve the biological activity of PMMA bone cement, which can also reduce the polymerization temperature by delaying the polymerization curing of methyl methacrylate (MMA) with the second phase[4-6].

Among various bioactive materials, bioactive glasses exhibit superior biocompatibility, bioactivity and biodegradability, because they can react with body fluid to generate hydroxyapatite to form a firm bond with bone and soft tissue, and their released ions can also stimulate angiogenesis and osteogenesis[7]. Previous studies indicated that the mesoporous borosilicate bioglass microspheres hold better bioactivity and biodegradability than do the traditional silicate bioglass because the increased specific surface area of porous bioglass leads to better surface reactivity and degradability[8-10]. Cui *et al*.[11] prepared strontium-doped borosilicate bioactive glass by melting method to improve the bioactivity and bone integration ability of PMMA bone cement.

However, the mechanical properties of composite bone cement decrease due to the lack of strong chemical bonding between hydrophilic inorganic particles and hydrophobic organic matrix[12]. The desirable mechanical properties of bone cement are essential for the long-term stability because they undertake the function of transferring load and providing mechanical support when used to repair load-bearing bone defects. By surface modification of bioactive glass through silane coupling agent, chemical bonding between bioactive glass and PMMA matrix can be established to improve the mechanical properties of

the composite bone cement[13]. In addition, silane coupling agents do not have intrinsic toxicity[14]. However, implementing surface modification to MBGS with silane coupling agents could change the microstructure, resulting in the loss of bioactivity. Nevertheless, the microstructure and bioactivity of MBGS effected by the silanization and the properties of PMMA based composite bone cement modified by MBGSSI have not been reported.

In this research, we prepared MBGS by template method and modified them by silane coupling agent γ-MPS to obtain MBGSSI. The constituents and microstructures of MBGS and MBGSSI were determined. MBGS and MBGSSI were combined with PMMA bone cement to prepare MBGS/PMMA and MBGSSI/PMMA composite bone cement, respectively, and the setting properties, mechanical properties and *in vitro* bioactivity were studied.

1　Materials and methods

1.1　Materials and reagents

Tributyl borate (TBB, CP), tetraethyl orthosilicate (TEOS, AR), calcium nitrate tetrahydrate (CN, AR), triethylphosphate (TEP, CP), cetyltrimethyl ammonium bromide (CTAB, AR), ammonia solution (25%, AR), γ-methylacryloxy propyltrimethoxysilane (γ-MPS, KH 570, ≥98.0%) and benzoyl peroxide (BPO, CP) were purchased from Sinopharm Chemical Reagent Co., LTd (China). Acetate (AR, 99.5%), methyl methacrylate (MMA, >99.5%) and *N, N*-dimethyl-*p*-toluidine (DMPT, >98.0%) were purchased from Shanghai Aladdin Bio-Chem Technology Co., LTD (China). Poly(methyl methacrylate) (PMMA) was purchased from Makevale Group (UK).

1.2　Material preparation

According to the previous study, MBGS were prepared by template method using TBB, TEOS, CN, and TEP as raw materials to obtain the composition of $20B_2O_3$-$40SiO_2$-$36CaO$-$4P_2O_5$[15]. CTAB was used as template and $NH_3·H_2O$ was used as catalyst. The reaction was carried out at 40 ℃ with a stirring rate of 400 r/min. 0.15 g CTAB was dissolved in a mixture containing 80 mL deionized water and 40 mL absolute ethanol under stirring for 30 min. Then 1.629 mL TEOS was added into the solution. After stirred for 10 min, 1 mL ammonia solution was added as a catalyst and stirred for 10 min. Subsequently 1.946 mL TBB and 0.248 mL TEP were added and stirred for 30 min. Thereafter, 1.546 g CN was added into the solution and stirred for 3 h. The micro-spheres were separated by centrifugation, washed by absolute ethanol, deionized water and absolute ethanol successively, and dried at 60 ℃ in the oven.

Finally, MBGS were obtained after heat treatment at 450 ℃ for 5 h at a rate of 1 ℃/min.

Based on references, we developed silanation process to modify MBGS[16-18]. The silanization of MBGS by γ-MPS was carried out at 65 ℃ with a stirring rate of 400 r/min. 2 mL γ-MPS was added into a mixture containing 20 mL deionized water and 80 mL absolute ethanol, with pH being regulated at about 4.5 by acetate. After stirring for 30 min, 2 g MBGS was added into the solution, maitaining the reaction for 2 h. The microspheres were separated by centrifugation, washed by absolute ethanol and dried at 60 ℃. Finally, the products were treated at 100 ℃ for 2 h at a rate of 1 ℃/min to obtain MBGSSI.

The solid phase of MBGS/PMMA composite bone cement is composed of 2 g PMMA powder, 0.4 g MBGS and 0.5% BPO, while the liquid phase contains 1 mL MMA and 0.6% DMPT. Their solid or liquid phase were mixed and stirred at 23 ℃ and cured in the mold to obtain MBGS/PMMA according to ISO 5833:2002[19]. MBGSSI/PMMA was prepared by the same steps.

1.3　Characterization

MBGS and MBGSSI were characterized by X-ray Diffraction (XRD, D/max2550, Japan) at a scanning rate of 5 (°)/min in the range of 10°–80°, Fourier Transform Infrared Spectroscopy (FT-IR, EQUINOXSS, Germany), Thermogravimetric Analyzer (TA, Q600, USA) from 30 ℃ to 800 ℃ at a heating rate of 10 ℃/min, high resolution Transmission Electron Microscope (TEM, H-800, Japan), specific surface area analyzer (BET, CHA-SA, China), and X-ray Photoelectron Spectrometer (XPS, ESCALAB 250XI, USA).

Setting properties and mechanical properties of PMMA, MBGS/PMMA and MBGSSI/PMMA bone cements were tested according to ISO 5833:2002 by Paperless Recorder (STR3101, China) and Electronic Universal Testing Machine (CTM2500, China).

Bone cements were observed by Field Emission Scanning Electron Microscope (SEM, Tuanta 200 FEG, USA) and analyzed by Energy Dispersive Spectroscope (EDS, Tuanta 200 FEG, USA) and X-ray Diffraction (XRD, D/max2550, Japan).

2　Results and discussion

2.1　Microstructures and constituents of MBGS and MBGSSI

Phase and chemical composition of MBGS and MBGSSI were explored with XRD, FT-IR and TG measurement (Fig. 1 (a-c)). There is no sharp diffraction peak in the XRD patterns of MBGS and MBGSSI,

indicating that the silanization does not change the amorphous phase of the bioglass. The FT-IR spectrum of MBGSSI exhibits peaks belong to both MBGS and γ-MPS, demonstrating the presence of γ-MPS in MBGSSI[20-22]. The MBGSSI are composed of about 95% inorganic composition and 5% organic composition (Fig. 1 (c)). Major decomposition of γ-MPS takes place between 100 and 200 ℃, while weight loss of MBGSSI is accelerated at 300 ℃ due to the strong chemical bond being formed between γ-MPS and bioglass[17].

Microstructures of MBGS and MBGSSI (Fig. 1 (d, e)) consolidate a spherical structure with a diameter of about 450 nm and numerous pores, while MBGSSI show denser microstructures because γ-MPS enters the pore and binds with MBGS[23].

According to the result of N_2 adsorption-desorption isotherm and corresponding pore size distribution, the pore structure of MBGS and MBGSSI was analyzed by BET method (Fig. 2(a, b)). Hysteresis loop back indicates their mesoporous structure (Fig. 2(a)). Pore
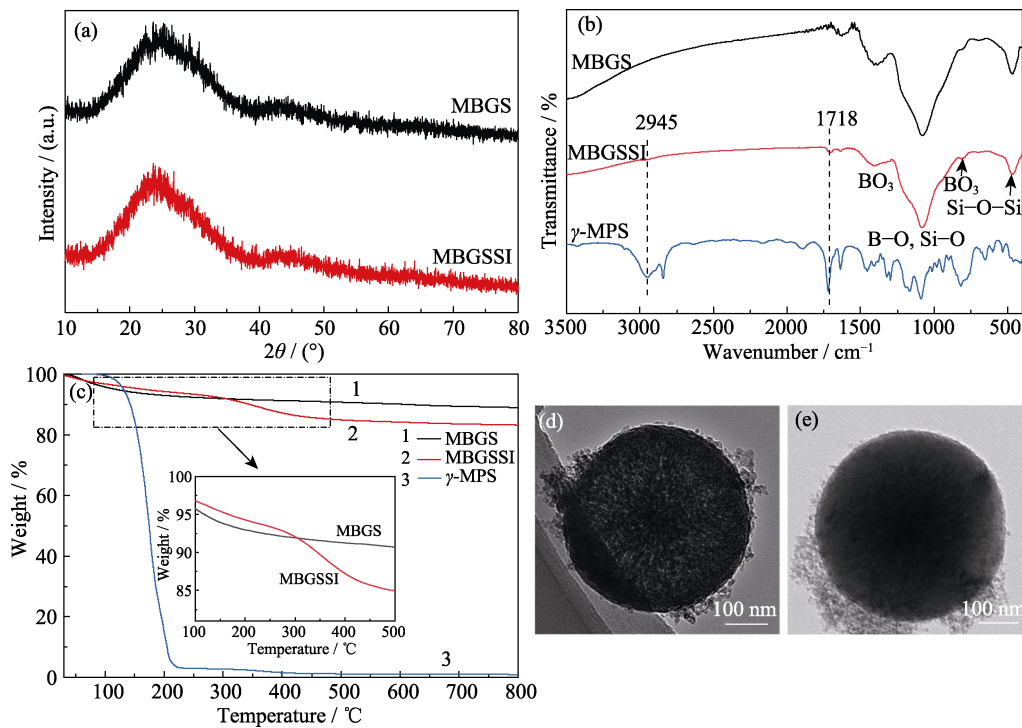

Fig. 1　Microstructures and constituents of MBGS and MBGSSI

(a) XRD patterns of MBGS and MBGSSI; (b, c) FT-IR spectra (b) and TG curves (c) of MBGS, MBGSSI and γ-MPS; (d, e) TEM images of MBGS (d) and MBGSSI (e)
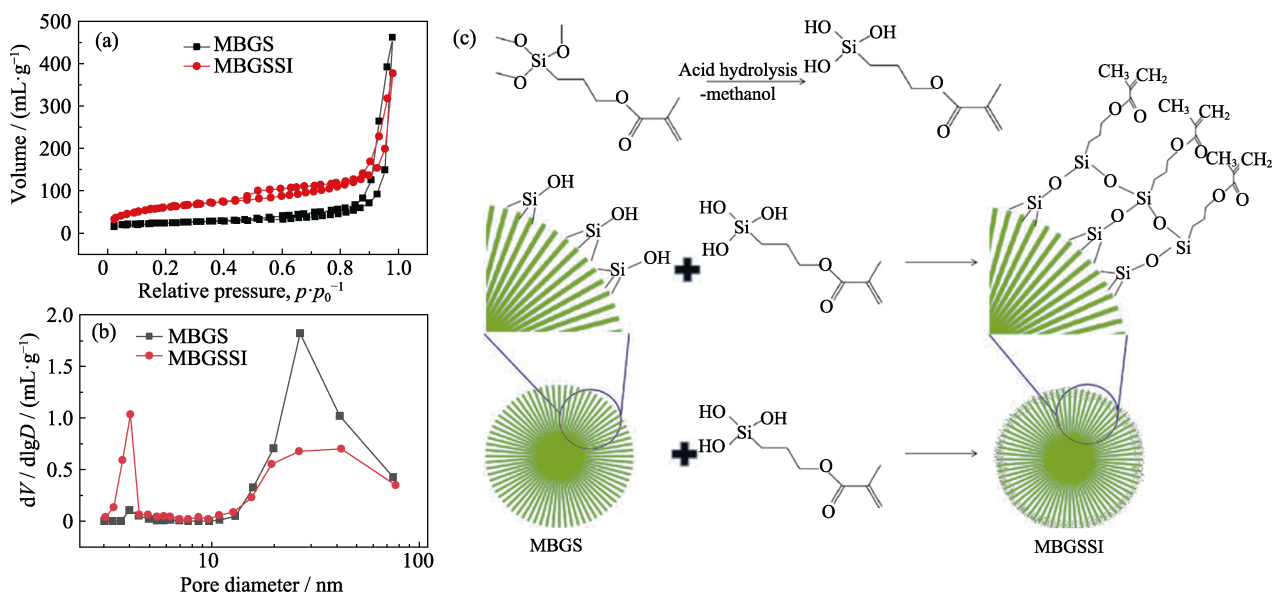

Fig. 2　(a) N_2 adsorption-desorption isotherms and (b) corresponding pore size distributions of MBGS, and (c) schematic diagram of the surface silanization

diameter of MBGS is mainly distributed between 13–50 nm, while pore diameter of MBGSSI presents a large differentiation, with a large number of distributions between 3–5 nm and 13–50 nm (Fig. 2(b)). The distribution of pore diameter proves that modifying MBGS with γ-MPS results in decrease of large pores and increase of small pores, leading to drastic increase of specific surface area. Besides, there exists a large number of larger pores (>50 nm) due to microspheres accumulation, evidenced by obvious N_2 adsorption in the high pressure area (Fig. 2(a)). Specific surface area, average pore diameter and total pore volume of MBGS and MBGSSI were compared in Table 1. As the schematic diagram of surface modification shown, γ-MPS binds to Si–OH on the surface of MBGS (Fig. 2(c)), causing a significant increase of specific surface area and decreases of average pore diameter and total pore volume because γ-MPS occupies a certain volume[24].

XPS survey spectra of MBGS and MBGSSI prove the existence of γ-MPS on the surface of MBGSSI (Fig. 3(a)). It can be further observed (Fig. 3(b, c)) that atomic percentage of C1s C=O on MBGSSI decreases from 1.11% to 0.32% as etching depth increases from 0 to 100 nm, demonstrating that the binding between γ-MPS and MBGS mainly occurs on the near surface of mesoporous microspheres. Atomic concentrations of MBGS, MBGSSI and MBGSSI (etching depth at 100 nm) were compared in Table 2.

2.2 Setting properties and mechanical properties of bone cements

The setting properties and mechanical properties of PMMA, MBGS/PMMA and MBGSSI/PMMA bone cements were summarized in Table 3. Compared with PMMA, MBGS/PMMA and MBGSSI/PMMA show shorter

dough time and longer setting time that are beneficial for clinical operation due to the rise of solid/liquid and decrease of organic concentration in the composite. In addition, polymerization curing is prolonged by addition of the second phase, resulting in lower peak temperature which also benefits clinical application.

However, after adding MBGS in PMMA, the flexural strength of bone cement significantly decreases to (44.53±2.59) MPa, which is lower than the standard strength of ISO 5833:2002 ($\geqslant$50 MPa)[19]. This is because physical mixture between hydrophilic bioglass and hydrophobic PMMA results in agglomeration of inorganic phase in the organic matrix, and brittle fracture was caused by stress concentration in the test of bending resistance[25-26]. While allyl oxy group in γ-MPS reacts with C=C in MMA monomer, whose strong chemical bond makes the inorganic phase dispersed evenly in the organic matrix, leading to better flexural strength of MBGSSI/PMMA[27]. In addition, the composite bone cements show increased compressive modulus and flexural modulus because the inorganic rigid mesoporous microspheres improve the ability of bone cements to resist the deformation[26].

Fig. 4 shows the dispersity of MBGS and MBGSSI in MMA monomer. MBGS settle obviously in 5 min, while MBGSSI disperse in the MMA for a longer period of time. Moreover, SEM images of PMMA, MBGS/PMMA and MBGSSI/PMMA bone cements (Fig. 5) show that MBGS on the surface of composite bone cement agglomerate, while MBGSSI disperse evenly in the organic matrix, which matching the mechanical properties of composite bone cements.

2.3 *In vitro* bioactivity of bone cements

After immersing in SBF for 42 d, morphologies of

Table 1 Specific surface area, average pore diameter and total pore volume of MBGS and MBGSSI

Sample	Specific surface area/(m²·g⁻¹)	Average pore diameter/nm	Total pore volume/(mL·g⁻¹)
MBGS	84.047	33.9676	0.7137
MBGSSI	227.856	10.22	0.5822

Table 2 Atomic concentrations of MBGS, MBGSSI and MBGSSI (etching depth at 100 nm)

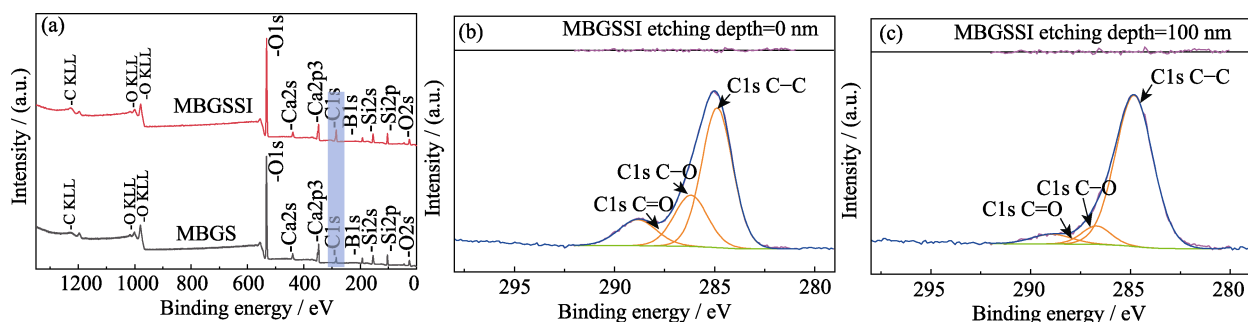| Sample	C1s/%	O1s/%	Si2p/%	B1s/%	Ca2p/%
MBGS	5.02	72.38	5.27	2.71	14.62
MBGSSI 0 nm	7.91	70.26	5.68	2.27	13.88
MBGSSI 100 nm	5.32	68.88	6.81	2.25	16.74

Fig. 3 (a) XPS spectra of MBGS and MBGSSI, XPS spectra of C1s in MBGSSI at etching depths of (b) 0 and (c) 100 nm

Table 3　Setting and mechanical properties of PMMA, MBGS/PMMA and MBGSSI/PMMA bone cements

| Sample	Dough time/s	Setting time/min	Peak temperature/℃	Compressive strength/MPa	Compressive modulus/MPa	Flexural strength/MPa	Flexural modulus/MPa
PMMA	287.5±7.8	11.38±0.37	49.15±1.45	70.01±1.85	878.67±55.84	67.75±1.88	2925.05±144.71
MBGS/PMMA	136.0±2.8	14.77±0.07	40.65±0.25	71.22±2.20	1029.66±63.54	44.53±2.59	4003.19±125.79
MBGSSI/PMMA	174.0±5.7	18.97±0.20	38.40±0.4	81.77±1.45	1091.50±75.64	59.42±4.34	3330.03±214.02
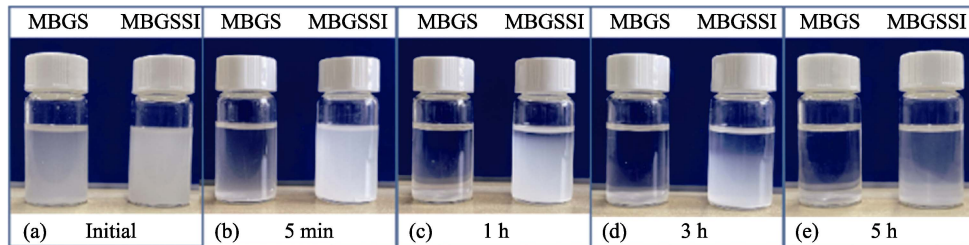
Fig. 4　Dispersity of MBGS and MBGSSI in MMA at (a) initial or for (b) 5 min, (c) 1 h, (d) 3 h and (e) 5 h
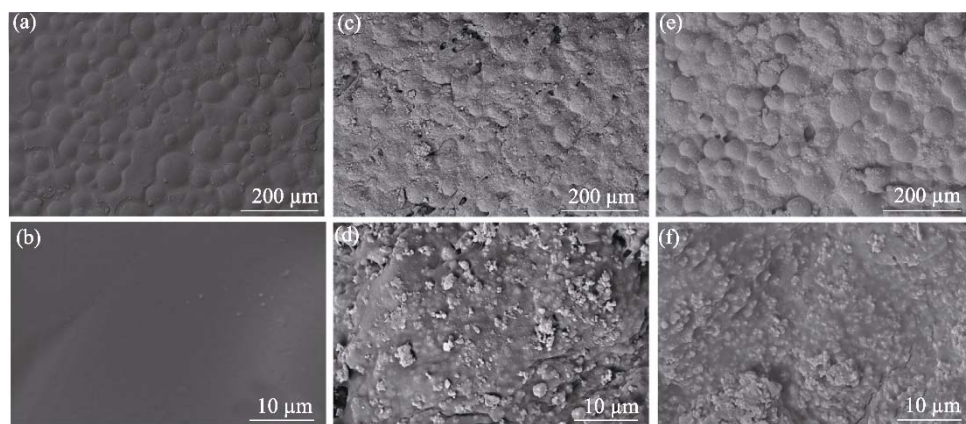

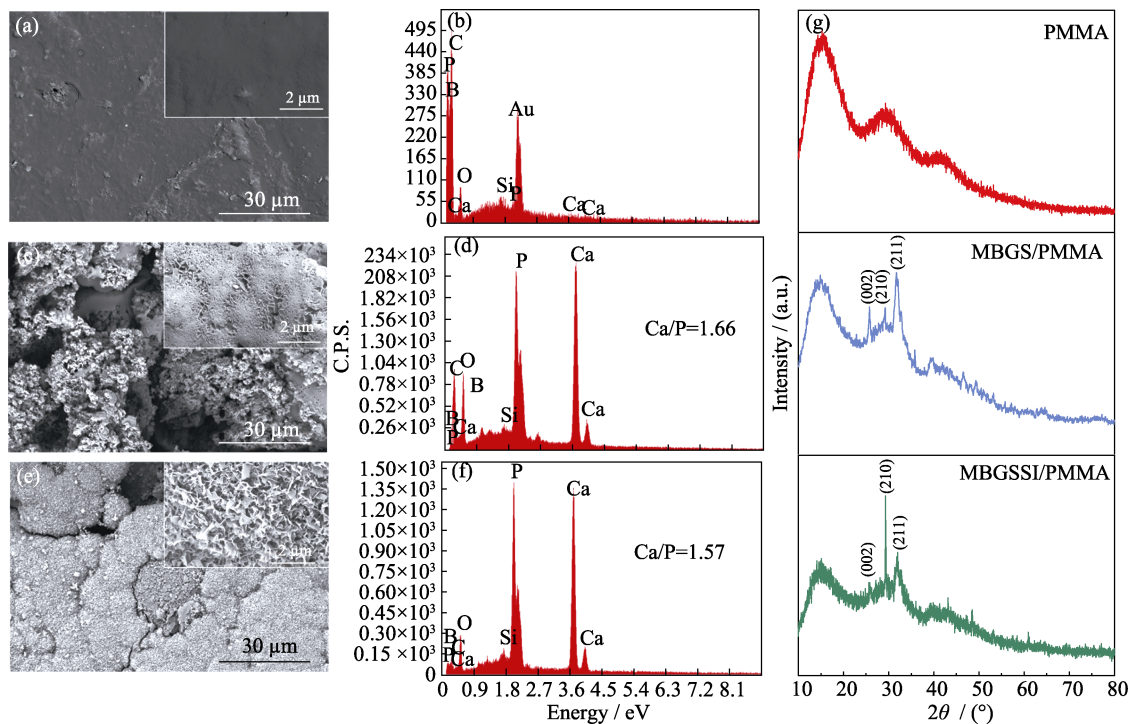Fig. 5　SEM images of (a, b) PMMA, (c, d) MBGS/PMMA and (e, f) MBGSSI/PMMA

Fig. 6　SEM images and EDS patterns of (a, b) PMMA, (c, d) MBGS/PMMA and (e, f) MBGSSI/PMMA, and (g) XRD patterns of PMMA, MBGS/PMMA, MBGSSI/PMMA

PMMA, MBGS/PMMA and MBGSSI/PMMA bone cements were characterized by SEM, EDS and XRD measurements. As can be observed that dense lamellar structure appears on the surface of MBGS/PMMA and MBGSSI/PMMA, while the surface of pure PMMA still keeps smooth (Fig. 6(a, c, e)). The diffraction peaks corresponding to (002), (210) and (211) of HA (PDF#09-0432) can be observed in the XRD patterns of MBGS/PMMA and MBGSSI/PMMA (Fig. 6(g)), indicating HA being formed on the surfaces of composite bone cements. This result proves the excellent *in vitro* bioactivity of MBGS/PMMA and MBGSSI/PMMA. Moreover, the lower element content ratio of Ca and P of MBGSSI/PMMA studied by EDS indicates that formation of calcium-deficient hydroxyapatite, which is caused by the limited ion dissolution of MBGSSI due to the silane modification.

3　Conclusions

MBGS with high specific surface area were successfully prepared by template method and then modified by γ-MPS to obtain MBGSSI. BET and XPS results indicates that the binding between γ-MPS and MBGS mainly occurs on the near surface of mesoporous microspheres, resulting in the increase of specific surface area and decrease of average pore diameter and total pore volume. Moreover, the silanization improves the bonding between hydrophilic bioglass and hydrophobic organic PMMA matrix. Hence, MBGSSI/PMMA composite bone cement presents suitable setting properties and improved mechanical properties compared with MBGS/PMMA. In addition, MBGSSI/PMMA shows excellent *in vitro* bioactivity, which can be a promising bone repair material.

References:

[1] SHRIDHAR P, CHEN Y, KHALIL R, *et al.* A review of PMMA bone cement and intra-cardiac embolism. *Materials*, 2016, **9(10):** 821.

[2] GLADIUS L. Alternative acrylic bone cement formulations for cemented arthroplasties: present status, key issues, and future prospects. *Journal of Biomedical Materials Research. Part B, Applied Biomaterials*, 2008, **84(2):** 301.

[3] ZHU J J, JIANG G Q, QIU Z Y, *et al.* Modification of poly(methyl methacrylate) bone cement for vertebroplasty. *Journal of Bioma-terials and Tissue Engineering*, 2018, **8(5):** 607.

[4] CHEN L, ZHAI D, HUAN Z G, *et al.* Silicate bioceramic/PMMA composite bone cement with distinctive physicochemical and bioactive properties. *RSC Advances*, 2015, **5(47):** 37314.

[5] SA Y, YANG F, WIJN J R D, *et al.* Physicochemical properties and mineralization assessment of porous polymethylmethacrylate cement loaded with hydroxyapatite in simulated body fluid. *Materials Science & Engineering C*, 2016, **61:** 190.

[6] FERREIRA B J M L, BARROCA N B, LOPES P P, *et al.* Properties of novel PMMA-co-EHA bone cements filled with

hydroxyapatite. *Polymer Composites*, 2014, **35(4):** 759.

[7] SERGI R, BELLUCCI D, CANNILLO V. A comprehensive review of bioactive glass coatings: state of the art, challenges and future perspectives. *Coatings*, 2020, **10(8):** 757.

[8] BAINO F, FIUME E, MIOLA M, *et al.* Bioactive Sol-Gel glasses: processing, properties, and applications. *International Journal of Applied Ceramic Technology*, 2018, **15(4):** 841.

[9] LI Y, CHEN X, NING C, *et al.* Facile synthesis of mesoporous bioactive glasses with controlled shapes. *Materials Letters*, 2015, **161:** 605.

[10] ZHONG J P, GREENSPAN D C. Processing and properties of Sol-Gel bioactive glasses. *Journal of Biomedical Materials Research*, 2000, **53(6):** 694.

[11] CUI X, HUANG C C, ZHANG M, *et al.* Enhanced osteointegra-tion of poly(methylmethacrylate) bone cements by incorporating strontium-containing borate bioactive glass. *Journal of the Royal Society Interface*, 2017, **14(131):** 20161057.

[12] BOLAINA-LORENZO E D, CERVANTES-UC J M, CAUICH-RODRIGUEZ J V, *et al.* Effect of barium sulfate surface treatments on the mechanical properties of acrylic bone cements. *Polymer Bulletin*, 2020, **78(3):** 1.

[13] DEBNATH S, RANADE R, WUNDER S L, *et al.* Interface effects on mechanical properties of particle-reinforced composites. *Dental Materials: Official Publication of the Academy of Dental Materials*, 2004, **20(7):** 677.

[14] LUNG C Y K, MATINLINNA J P. Aspects of silane coupling agents and surface conditioning in dentistry: an overview. *Dental Materials*, 2012, **28(5):** 467.

[15] CHANG Y C, LIN Z Y, XIE X, *et al.* An injectable composite bone cement based on mesoporous borosilicate bioactive glass spheres *Journal of Inorganic Materials*, 2020, **35(12):** 1398.

[16] MATINLINNA J P, LUNG C Y K, TSOI J K H. Silane adhesion mechanism in dental applications and surface treatments: a review. *Dental Materials*, 2018, **34(1):** 13.

[17] ALONSO L M, GARCIA-MENOCAL J A, AYMERICH M T, *et al.* Calcium phosphate glasses: silanation process and effect on the bioactivity behavior of glass-PMMA composites. *Journal of Biomedical Materials Research. Part B, Applied Biomaterials*, 2014, **102(2):** 205.

[18] SALON M C B, BAYLE P A, ABDELMOULEH M, *et al.* Kinetics of hydrolysis and self condensation reactions of silanes by NMR spectroscopy. *Colloids and Surfaces a-Physicochemical and Engineering Aspects*, 2008, **312(2):** 83.

[19] ISO member body. Implants for Surgery-Acrylic Resin Cements. International Standard. ISO5833: 2002. Switzerland: ISO organiza-tion-(IX-ISO), 2002.

[20] LIU X, RAHAMAN M N, DAY D E. Conversion of melt-derived microfibrous borate (13-93B3) and silicate (45S5) bioactive glass in a simulated body fluid. *Journal of Materials Science. Materials in Medicine*, 2013, **24(3):** 583.

[21] ALI A A, RAMMAH Y S, EL-MALLAWANY R, *et al.* FTIR and UV spectra of pentaternary borate glasses. *Measurement*, 2017, **105:** 72.

[22] ZAGRAJCZUK B, DZIADEK M, OLEJNICZAK Z, *et al.* Structural and chemical investigation of the gel-derived bioactive materials from the SiO₂-CaO and SiO₂-CaO-P₂O₅ systems. *Ceramics International*, 2017, **43(15):** 12742.

[23] DOU B J, HU Q, LI J J, *et al.* Adsorption performance of VOCs in ordered mesoporous silicas with different pore structures and surface chemistry. *Journal of Hazardous Materials*, 2011, **186(2/3):** 1615.

[24] CHEN Z D, MA Y X, GOU L A, *et al.* Construction of caffeic acid modified porous starch as the dual-functional microcapsule for

encapsulation and antioxidant property. *International Journal of Biological Macromolecules*, 2022, **228:** 358.

[25] CHRISTIAN H, V B D, BRIAN Y, *et al.* Polymer nanocomposites having a high filler content: synthesis, structures, properties, and applications. *Nanoscale*, 2019, **11(11):** 4653.

[26] ALDABIB J M, ISHAK Z A M. Effect of hydroxyapatite filler concentration on mechanical properties of poly (methyl methacrylate) denture base. *SN Applied Sciences*, 2020, **2:** 732.

[27] KINLOCH A J. Adhesion and adhesives: science and technology: London: Chapman and Hall, 1987: 171–187.

硅烷化介孔硼硅酸盐生物玻璃微球对 PMMA 骨水泥生物活性和力学性能的影响

倪晓诗，林子扬，秦沐严，叶 松，王德平

(同济大学 材料科学与工程学院，上海 201804)

摘 要：聚甲基丙烯酸甲酯(PMMA)骨水泥因具有良好的力学性能、适宜的凝固时间和低毒性等优点而在骨科手术中作为可注射型人工骨修复材料受到广泛的应用。然而，其生物惰性可能导致假体长期植入后产生无菌性松动。本研究采用模板法制备了介孔硼硅酸盐生物玻璃微球(MBGS)，并用硅烷偶联剂 γ-甲基丙烯酰氧基丙基三甲氧基硅烷(γ-MPS)对其进行改性，制备了 MBGSSI。再将硅烷化介孔硼硅酸盐生物玻璃微球(MBGSSI)与聚甲基丙烯酸甲酯(PMMA)骨水泥复合，制备了一种具有良好生物活性和力学性能的复合骨水泥。实验结果表明，由于 γ-MPS 与 MBGS 的结合主要发生在介孔微球的近表面，MBGSSI 比 MBGS 具有更大的比表面积和更小的孔容积。与 MBGS/PMMA 复合骨水泥相比，γ-MPS 可以改善复合材料中无机相和有机相之间的结合，因此 MBGSSI/PMMA 复合骨水泥的力学性能得到了改善，符合 ISO 5833:2002 对丙烯酸类骨水泥的力学性能要求。此外，在 SBF 溶液中浸泡42 d 后，MBGS/PMMA 和 MBGSSI/PMMA 复合骨水泥的表面均生成了羟基磷灰石(HA)，证明复合骨水泥具有良好的生物活性。因此, MBGSSI/PMMA 复合骨水泥是一种潜在的骨修复材料。

关 键 词：生物玻璃；硅烷化；PMMA 骨水泥；生物活性；力学性能

中图分类号：R318 **文献标志码：**A